Available online at www.sciencedirect.com

ScienceDirect

Nuclear Physics B 791 (2008) 1–19

NUCLEAR PHYSICS B

Higgs boson production at the LHC: Transverse-momentum resummation and rapidity dependence

Giuseppe Bozzi [a], Stefano Catani [b], Daniel de Florian [c], Massimiliano Grazzini [b,*]

[a] *Institut für Theoretische Physik, Universität Karlsruhe, PO Box 6980, D-76128 Karlsruhe, Germany*
[b] *INFN, Sezione di Firenze and Dipartimento di Fisica, Università di Firenze, I-50019 Sesto Fiorentino, Florence, Italy*
[c] *Departamento de Física, Facultad de Ciencias Exactas y Naturales, Universidad de Buenos Aires, (1428) Pabellón 1 Ciudad Universitaria, Capital Federal, Argentina*

Received 30 May 2007; accepted 24 September 2007

Available online 10 October 2007

This paper is dedicated to the memory of Jiro Kodaira, great friend and distinguished colleague

Abstract

We consider Higgs boson production by gluon fusion in hadron collisions. We study the doubly-differential transverse-momentum (q_T) and rapidity (y) distribution of the Higgs boson in perturbative QCD. In the region of small q_T $(q_T \ll M_H$, M_H being the mass of the Higgs boson), we include the effect of logarithmically-enhanced contributions due to multiparton radiation to all perturbative orders. We use the impact parameter and double Mellin moments to implement and factorize the multiparton kinematics constraint of transverse- and longitudinal-momentum conservation. The logarithmic terms are then systematically resummed in exponential form. At small q_T, we perform the all-order resummation of large logarithms up to next-to-next-to-leading logarithmic accuracy, while at large q_T $(q_T \sim M_H)$, we apply a matching procedure that recovers the fixed-order perturbation theory up to next-to-leading order. We present quantitative results for the differential cross section in q_T and y at the LHC, and we comment on the comparison with the q_T cross section integrated over y.

PACS: 12.38.Cy; 14.80.Bn

Keywords: Higgs; QCD; Hadronic colliders; LHC

* Corresponding author.
E-mail address: massimiliano.grazzini@cern.ch (M. Grazzini).

doi:10.1016/j.nuclphysb.2007.09.034

1. Introduction

The search for the Higgs boson [1] and the study of its properties (mass, couplings, decay widths) at hadron colliders require a detailed understanding of its production mechanisms. This demands reliable computations of related quantities, such as production cross sections and the associated distributions in rapidity and transverse momentum. In this paper we consider the production of the Standard Model (SM) Higgs boson by the gluon fusion mechanism.

The gluon fusion process $gg \to H$, through a heavy-quark (mainly, top-quark) loop, is the main production mechanism of the SM Higgs boson H at hadron colliders. When combined with the decay channels $H \to \gamma\gamma$ and $H \to ZZ$, this production mechanism is one of the most important for Higgs boson searches and studies over the entire range, $100\ \text{GeV} \lesssim M_H \lesssim 1\ \text{TeV}$, of Higgs boson mass M_H to be investigated at the LHC [2]. In the mass range $140\ \text{GeV} \lesssim M_H \lesssim 180\ \text{GeV}$, the gluon fusion process, followed by the decay $H \to WW \to \ell^+\ell^-\nu\bar{\nu}$, can be exploited as main discovery channel at the LHC and also at the Tevatron [3], provided the background from $t\bar{t}$ production is suppressed by applying a veto cut on the transverse momenta of the jets accompanying the final-state leptons.

The dynamics of the gluon fusion mechanism is controlled by strong interactions. Detailed studies of the effect of QCD radiative corrections are thus necessary to obtain accurate theoretical predictions.

In QCD perturbation theory, the leading order (LO) contribution to the total cross section for Higgs boson production by gluon fusion is proportional to α_S^2, α_S being the QCD coupling. The QCD radiative corrections to the total cross section are known at the next-to-leading order (NLO) [4–7] and at the next-to-next-to-leading order (NNLO) [8–12]. The Higgs boson rapidity distribution is also known at the NLO [13] and at the NNLO [14,15]. The effects of a jet veto have been studied up to the NNLO [11,14,15]. We recall that all the results at NNLO have been obtained by using the large-M_t approximation, M_t being the mass of the top quark. This approximation is justified by the fact that the bulk of the QCD radiative corrections to the total cross section is due to virtual and soft-gluon contributions [9–11,16,17]. The soft-gluon dominance also implies that higher-order perturbative contributions can reliably be estimated by applying resummation methods [9] of *threshold logarithms*, a type of logarithmically-enhanced terms due to multiple soft-gluon emission. In Ref. [17], the NNLO calculation of the total cross section is supplemented with threshold resummation at the next-to-next-to-leading logarithmic (NNLL) level; the residual perturbative uncertainty at the LHC is estimated to be at the level of better than $\pm 10\%$. The NNLL + NNLO results [17] are nicely confirmed by the more recent computation [18–20] of the soft-gluon terms at N^3LO; the quantitative effect [18] of the additional (i.e., beyond the NNLL order) single-logarithmic term at N^3LO is consistent with the estimated uncertainty at NNLL + NNLO. The effect of threshold logarithms on the rapidity distribution of the Higgs boson has been considered in Ref. [21].

The gluon fusion mechanism at $\mathcal{O}(\alpha_S^2)$ produces a Higgs boson with a vanishing transverse momentum q_T. A large (or, however, non-vanishing) value of q_T can be obtained only starting from $\mathcal{O}(\alpha_S^3)$, when the Higgs boson is accompanied by at least one recoiling parton in the final state. This mismatch by a power of α_S is a preliminary indication of the fact that the small-q_T and large-q_T regions are controlled by different dynamics regimes.

The large-q_T region is identified by the condition $q_T \sim M_H$. In this region, the perturbative series is controlled by a small expansion parameter, $\alpha_S(M_H^2)$, and calculations based on the truncation of the series at a fixed order in α_S are theoretically justified. The LO, i.e., $\mathcal{O}(\alpha_S^3)$, calculation is reported in Ref. [22]. The results of Ref. [22] and the higher-order studies of Refs. [23, 24] show that the large-M_t approximation is sufficiently accurate also in the case of the q_T distribution when $q_T \lesssim M_H$, provided $q_T \lesssim M_t$. Using the large-M_t approximation, the NLO QCD computation of the q_T distribution of the SM Higgs boson is presented in Refs. [14,15,25–27]. QCD corrections beyond the NLO are evaluated in Ref. [28], by implementing threshold resummation at the next-to-leading logarithmic (NLL) level. The results of the numerical programs of Refs. [14,15] can also be safely (i.e., without encountering infrared divergences) extended from large values of q_T to $q_T = 0$: in the small-q_T region these programs evaluate the q_T distribution up to NNLO.

In the small-q_T region ($q_T \ll M_H$), where the bulk of events is produced, the convergence of the fixed-order expansion is definitely spoiled, since the coefficients of the perturbative series in $\alpha_S(M_H^2)$ are enhanced by powers of large logarithmic terms, $\ln^m(M_H^2/q_T^2)$. The logarithmic terms are produced by multiple emission of soft and collinear partons (i.e., partons with low transverse momentum). To obtain reliable perturbative predictions, these terms have to be resummed to all orders in α_S. The method to systematically perform all-order resummation of classes of logarithmically-enhanced terms at small q_T is known [29–36]. In the case of the SM Higgs boson, resummation has been explicitly worked out at leading logarithmic (LL), NLL [35, 37] and NNLL [38] level.

The fixed-order and resummed approaches at small and large values of q_T can then be matched at intermediate values of q_T, to obtain QCD predictions for the entire range of transverse momenta. Phenomenological studies of the SM Higgs boson q_T distribution at the LHC have been performed in Refs. [39–45], by combining resummed and fixed-order perturbation theory at different levels of theoretical accuracy. Other recent studies of various kinematical distributions of the SM Higgs boson at the LHC are presented in Refs. [46–50].

In Refs. [41,44] we studied the Higgs boson q_T distribution integrated over the rapidity. In the small-q_T region, the logarithmic terms were systematically resummed in exponential form by working in impact-parameter and Mellin-moment space. A constraint of perturbative unitarity was imposed on the resummed terms, to the purpose of reducing the effect of unjustified higher-order contributions at large values of q_T and, especially, at intermediate values of q_T. This constraint thus decreases the uncertainty in the matching procedure of the resummed and fixed-order contributions. Our best theoretical predictions were obtained by matching NNLL resummation at small q_T and NLO perturbation theory at large q_T. NNLL resummation includes the complete NNLO result at small q_T, and the unitarity constraint assures that the total cross section at NNLO is recovered upon integration over q_T of the transverse-momentum spectrum. Considering SM Higgs boson production at the LHC, we concluded [44] that the residual perturbative QCD uncertainty of the NNLL + NLO result is uniformly of about $\pm 10\%$ from small to intermediate values of transverse momenta.

In this paper we extend our study to include the dependence on the rapidity of the Higgs boson. Using the impact parameter and *double* Mellin moments, we can perform the extension by maintaining all the main features of the resummation formalism of Refs. [36,44]. We are then able to present results up to NNLL + NLO accuracy for the doubly-differential cross section in q_T and rapidity at the LHC.

The paper is organized as follows. In Section 2 we recall the main aspects of the resummation formalism, and we illustrate the steps that are necessary to include the dependence on the rapidity in the q_T resummed formulae. In Section 3 we apply the formalism to the production of the SM Higgs boson at the LHC, and we perform quantitative studies on the q_T and rapidity dependence of the doubly-differential cross section. Some concluding remarks are presented in Section 4.

Additional technical details on the double Mellin moments of the resummation formulae are given in Appendix A.

2. Rapidity dependence in q_T resummation

We consider the inclusive hard-scattering process

$$h_1(p_1) + h_2(p_2) \to H(y, q_T, M_H) + X, \tag{1}$$

where the collision of the two hadrons h_1 and h_2 with momenta p_1 and p_2 produces the Higgs boson H, accompanied by an arbitrary and undetected final state X. The centre-of-mass energy of the colliding hadrons is denoted by $\sqrt{s}$. The rapidity, y, of the Higgs boson is defined in the centre-of-mass frame of the colliding hadrons, and the forward direction ($y > 0$) is identified by the direction of the momentum p_1.

According to the QCD factorization theorem, the doubly-differential cross section for this process is

$$\frac{d\sigma}{dy\,dq_T^2}(y, q_T, M_H, s) = \sum_{a_1,a_2} \int_0^1 dx_1 \int_0^1 dx_2\, f_{a_1/h_1}\big(x_1, \mu_F^2\big) f_{a_2/h_2}\big(x_2, \mu_F^2\big) \times \frac{d\hat{\sigma}_{a_1a_2}}{d\hat{y}\,dq_T^2}\big(\hat{y}, q_T, M_H, \hat{s}; \alpha_S\big(\mu_R^2\big), \mu_R^2, \mu_F^2\big), \tag{2}$$

where $f_{a/h}(x, \mu_F^2)$ ($a = q_f, \bar{q}_f, g$) are the parton densities of the colliding hadrons at the factorization scale μ_F, $d\hat{\sigma}_{ab}$ are the partonic cross sections, and μ_R is the renormalization scale. Throughout the paper we use parton densities as defined in the $\overline{\mathrm{MS}}$ factorization scheme, and $\alpha_S(q^2)$ is the QCD running coupling in the $\overline{\mathrm{MS}}$ renormalization scheme. The rapidity, $\hat{y}$, and the centre-of-mass energy, $\hat{s}$, of the partonic cross section (subprocess) are related to the corresponding hadronic variables y and s:

$$\hat{y} = y - \frac{1}{2}\ln\frac{x_1}{x_2}, \qquad \hat{s} = x_1 x_2 s, \tag{3}$$

with the kinematical boundary $|\hat{y}| < \ln\sqrt{\hat{s}/M^2}$ ($|y| < \ln\sqrt{s/M^2}$) and $\hat{s} > M^2$ ($s > M^2$).

The partonic cross section $d\hat{\sigma}_{ab}$ is computable in QCD perturbation theory. Its power series expansion in α_S contains the logarithmically-enhanced terms, $(\alpha_S^n/q_T^2)\ln^m(M_H^2/q_T^2)$, that we want to resum. To this purpose, we use the general (process-independent) strategy and the formalism described in detail in Ref. [44]. The only difference with respect to Ref. [44] is that the resummation is now performed at fixed values of the rapidity y, rather than after integration over the rapidity phase space. In the following we briefly recall the main steps of the resummation formalism, and we point out explicitly the differences with respect to Ref. [44].

We first rewrite (see Section 2.1 in Ref. [44]) the partonic cross section as the sum of two terms,

$$\frac{d\hat{\sigma}_{a_1a_2}}{d\hat{y}\,dq_T^2} = \frac{d\hat{\sigma}_{a_1a_2}^{(\mathrm{res.})}}{d\hat{y}\,dq_T^2} + \frac{d\hat{\sigma}_{a_1a_2}^{(\mathrm{fin.})}}{d\hat{y}\,dq_T^2}. \tag{4}$$

The logarithmically-enhanced contributions are embodied in the 'resummed' component $d\hat{\sigma}_{a_1a_2}^{(\mathrm{res.})}$. The 'finite' component $d\hat{\sigma}_{a_1a_2}^{(\mathrm{fin.})}$ is free of such contributions, and it can be computed by truncation of the perturbative series at a given fixed order (LO, NLO and so forth). In practice, after having evaluated $d\hat{\sigma}_{a_1a_2}$ and its resummed component at a given perturbative order, the finite component $d\hat{\sigma}^{(\mathrm{fin.})}_{a_1a_2}$ is obtained by the matching procedure described in Sections 2.1 and 2.4 of Ref. [44].

The resummation procedure of the logarithmic terms has to be carried out [30–34] in the impact-parameter space, to correctly take into account the kinematics constraint of transverse-momentum conservation. The resummed component of the partonic cross section is then obtained by performing the inverse Fourier (Bessel) transformation with respect to the impact parameter b. We write[1]

$$\frac{d\hat{\sigma}^{(\mathrm{res.})}_{a_1a_2}}{d\hat{y}\,dq_T^2}(\hat{y}, q_T, M_H, \hat{s}; \alpha_S) = \frac{M_H^2}{\hat{s}} \int_0^\infty db \frac{b}{2} J_0(bq_T) \mathcal{W}_{a_1a_2}(\hat{y}, b, M_H, \hat{s}; \alpha_S), \tag{5}$$

where $J_0(x)$ is the 0th-order Bessel function, and the factor $\mathcal{W}$ embodies the all-order dependence on the large logarithms $\ln(M_H b)^2$ at large b, which correspond to the q_T-space terms $\ln(M_H^2/q_T^2)$ (the limit $q_T \ll M_H$ corresponds to $M_H b \gg 1$, since b is the variable conjugate to q_T).

In the case of the q_T cross section integrated over the rapidity, the resummation of the large logarithms is better expressed [36,44] by defining the N-moments $\mathcal{W}_N$ of $\mathcal{W}$ with respect to $z = M_H^2/\hat{s}$ at fixed M_H. In the present case, where the rapidity is fixed, it is convenient (see, e.g., Refs. [51,52]) to consider 'double' (N_1, N_2)-moments with respect to the two variables $z_1 = e^{+\hat{y}} M_H/\sqrt{\hat{s}}$ and $z_2 = e^{-\hat{y}} M_H/\sqrt{\hat{s}}$ at fixed M_H (note that $0 < z_i < 1$). We thus introduce $\mathcal{W}^{(N_1,N_2)}$ as follows:

$$\mathcal{W}^{(N_1,N_2)}_{a_1a_2}(b, M_H; \alpha_S) = \int_0^1 dz_1\, z_1^{N_1-1} \int_0^1 dz_2\, z_2^{N_2-1} \mathcal{W}_{a_1a_2}(\hat{y}, b, M_H, \hat{s}; \alpha_S). \tag{6}$$

More generally, any function $h(y; z)$ of the variables y ($|y| < -\ln\sqrt{z}$) and z ($0 < z < 1$) can be considered as a function of the two variables $z_1 = e^{+y}\sqrt{z}$ and $z_2 = e^{-y}\sqrt{z}$. Thus, throughout the paper, the (N_1, N_2)-moments $h^{(N_1,N_2)}$ of the function $h(y; z)$ are defined as

$$h^{(N_1,N_2)} \equiv \int_0^1 dz_1\, z_1^{N_1-1} \int_0^1 dz_2\, z_2^{N_2-1} h(y; z), \quad \text{where } y = \frac{1}{2}\ln\frac{z_1}{z_2},\ z = z_1 z_2. \tag{7}$$

Note that the double Mellin moments can also be obtained (see, e.g., Ref. [53]) by introducing a Fourier transformation with respect to y (with conjugate variable $\nu = i(N_2 - N_1)$) and then performing a Mellin transformation with respect to z (with conjugate variable $N = (N_1 + N_2)/2$):

$$h^{(N_1,N_2)} = \int_0^1 dz\, z^{N-1} \int_{-\infty}^{+\infty} dy\, e^{i\nu y} h(y; z), \quad \text{where } N_1 = N + i\nu/2,\ N_2 = N - i\nu/2. \tag{8}$$

The convolution structure of the QCD factorization formula (2) is readily diagonalized by considering (N_1, N_2)-moments:

$$d\sigma^{(N_1,N_2)} = \sum_{a_1,a_2} f_{a_1/h_1,N_1+1} f_{a_2/h_2,N_2+1}\, d\hat{\sigma}^{(N_1,N_2)}_{a_1a_2}, \tag{9}$$

[1] In the following equations, the functional dependence on the scales μ_R and μ_F is understood.

where $f_{a/h,N} = \int_0^1 dx\, x^{N-1} f_{a/h}(x)$ are the customary N-moments of the parton distributions.

The use of Mellin moments also simplifies the resummation structure of the logarithmic terms in $d\hat{\sigma}_{a_1a_2}^{(\mathrm{res.})(N_1,N_2)}$. The perturbative factor $\mathcal{W}_{a_1a_2}^{(N_1,N_2)}$ can indeed be organized in exponential form as follows:

$$\mathcal{W}^{(N_1,N_2)}(b, M_H; \alpha_S) = \mathcal{H}^{(N_1,N_2)}(M_H, \alpha_S) \exp\{\mathcal{G}^{(N_1,N_2)}(\alpha_S, \tilde{L})\}, \tag{10}$$

where

$$\tilde{L} = \ln\left(\frac{M_H^2 b^2}{b_0^2} + 1\right), \tag{11}$$

$b_0 = 2e^{-\gamma_E}$ ($\gamma_E = 0.5772\ldots$ is the Euler number) and, to simplify the notation, the dependence on the flavour indices has been understood.

The structure of Eq. (10) is in close analogy to the cases of soft-gluon resummed calculations for hadronic event shapes in hard-scattering processes [54] and for threshold contributions to hadronic cross sections [51,55,56]. The function $\mathcal{H}^{(N_1,N_2)}$ (which is process *dependent*) does not depend on the impact parameter b and, therefore, its evaluation does not require resummation of large logarithmic terms. It can be expanded in powers of α_S as

$$\mathcal{H}^{(N_1,N_2)}(M_H, \alpha_S) = \sigma_0(\alpha_S, M_H)\left[1 + \frac{\alpha_S}{\pi}\mathcal{H}^{(N_1,N_2)(1)} + \left(\frac{\alpha_S}{\pi}\right)^2 \mathcal{H}^{(N_1,N_2)(2)} + \cdots\right], \tag{12}$$

where $\sigma_0(\alpha_S, M_H)$ is the lowest-order partonic cross section for Higgs boson production. The form factor $\exp\{\mathcal{G}\}$ is process *independent*[2]; it includes the complete dependence on b and, in particular, it contains all the terms that order-by-order in α_S are logarithmically divergent when $b \to \infty$. The functional dependence on b is expressed through the large logarithmic terms $\alpha_S^n \tilde{L}^m$ with $1 \leqslant m \leqslant 2n$. More importantly, all the logarithmic contributions to $\mathcal{G}$ with $n + 2 \leqslant m \leqslant 2n$ are vanishing. Thus, the exponent $\mathcal{G}$ can systematically be expanded in powers of α_S, at fixed value of $\lambda = \alpha_S \tilde{L}$, as follows:

$$\mathcal{G}^{(N_1,N_2)}(\alpha_S, \tilde{L}) = \tilde{L} g^{(1)}(\alpha_S \tilde{L}) + g^{(2)(N_1,N_2)}(\alpha_S \tilde{L}) + \frac{\alpha_S}{\pi} g^{(3)(N_1,N_2)}(\alpha_S \tilde{L}) + \cdots. \tag{13}$$

The term $\tilde{L} g^{(1)}$ collects the leading logarithmic (LL) contributions $\alpha_S^n \tilde{L}^{n+1}$; the function $g^{(2)}$ resums the next-to-leading logarithmic (NLL) contributions $\alpha_S^n \tilde{L}^n$; $g^{(3)}$ controls the next-to-next-to-leading logarithmic (NNLL) terms $\alpha_S^n \tilde{L}^{n-1}$, and so forth.

Note that we use the logarithmic variable $\tilde{L}$ (see Eq. (11)) to parametrize and organize the resummation of the large logarithms $\ln(M_H b)^2$. We recall the main motivations [44] for this choice. In the resummation region $M_H b \gg 1$, we have $\tilde{L} \sim \ln(M_H b)^2$ and the use of the variable $\tilde{L}$ is fully legitimate to arbitrary logarithmic accuracy. When $M_H b \ll 1$, we have $\tilde{L} \to 0$ (whereas[3] $\ln(M_H b)^2 \to \infty$!) and $\exp\{\mathcal{G}(\alpha_S, \tilde{L})\} \to 1$. Therefore, the use of $\tilde{L}$ reduces the effect

---

[2] More precisely, it depends only on the flavour of the colliding partons (see Appendix A).

[3] As shown in Appendix B of Ref. [44] (see Eqs. (131) and (132) therein), after inverse Fourier transformation to q_T space, the b-dependent functions $\ln^n(M_H b)^2$ and $\tilde{L}^n$ lead to quite different behaviours at large q_T. When $q_T \gg M_H$, the behaviour $(1/q_T^2)\ln^{n-1}(q_T/M_H)$ (which is not integrable when $q_T \to \infty$) produced by $\ln^n(M_H b)^2$ is damped (and made integrable) by the extra factor $\sqrt{q_T/M_H}\exp(-b_0 q_T/M_H)$ produced in the case of $\tilde{L}^n$.

produced by the resummed contributions in the small-b region (i.e., at large and intermediate values of q_T), where the large-b resummation approach is not justified. In particular, setting $b = 0$ (which corresponds to integrate over the entire q_T range) we have $\exp\{\mathcal{G}(\alpha_S, \tilde{L})\} = 1$: this property can be interpreted [44] as a constraint of perturbative unitarity on the total cross section; the dynamics of the all-order recoil effects, which are resummed in the form factor $\exp\{\mathcal{G}(\alpha_S, \tilde{L})\}$, produces a smearing of the fixed-order q_T distribution of the Higgs boson without affecting its total production rate.

The resummation formulae (10), (12) and (13) can be worked out at any given (and arbitrary) logarithmic accuracy since the functions $\mathcal{H}$ and $\mathcal{G}$ can explicitly be expressed (see Ref. [44]) in terms of few perturbatively-computable coefficients denoted by $A^{(n)}$, $B^{(n)}$, $H^{(n)}$, $C_N^{(n)}$, $\gamma_N^{(n)}$. The key role of these coefficients to fully determine the structure of transverse-momentum resummation was first formalized by Collins, Soper and Sterman [32,34,36]. The present status of the calculation of these coefficients for Higgs boson production is recalled in Section 3.

In the case of the q_T cross section integrated over the rapidity, Eq. (10) is still valid, provided the double (N_1, N_2)-moments are replaced by the corresponding single N-moments $\mathcal{W}_N, \mathcal{H}_N, \mathcal{G}_N$ (see Section 2.2 in Ref. [44]). The relation between double and single moments can easily be understood by inspection of Eqs. (6)–(8). We see that setting $\nu = 0$ in Eq. (8) is exactly equivalent to integrate the cross section over the rapidity. Therefore, the functions $\mathcal{W}_N$, $\mathcal{H}_N, \mathcal{G}_N$ in Ref. [44] are obtained by simply setting $N_1 = N_2 = N$ in the corresponding functions $\mathcal{W}^{(N_1,N_2)}, \mathcal{H}^{(N_1,N_2)}, \mathcal{G}^{(N_1,N_2)}$ of Eq. (10).

Moreover, from the results presented in Ref. [44], we can straightforwardly obtain the functions $\mathcal{H}^{(N_1,N_2)}$ and $\mathcal{G}^{(N_1,N_2)}$ from the functions $\mathcal{H}_N$ and $\mathcal{G}_N$. Roughly speaking, we simply have

$$\mathcal{G}^{(N_1,N_2)} = \frac{1}{2}(\mathcal{G}_{N_1} + \mathcal{G}_{N_2}), \qquad \mathcal{H}^{(N_1,N_2)} = [\mathcal{H}_{N_1}\mathcal{H}_{N_2}]^{1/2}. \tag{14}$$

More precisely, these equalities are valid in the simplified case where there is a single species of partons (e.g., only gluons). In the following we comment on the physical picture that leads to Eq. (14). The generalization to considering more species of partons does not require any further conceptual steps: it just involves algebraic complications related to the treatment of the flavour indices. The multiflavour case is briefly illustrated in Appendix A.

In the small-q_T (large-b) region that we are considering, the kinematics of the Higgs boson is fully determined by the radiation of soft and collinear partons from the colliding partons (hadrons) in the initial state. The radiation of soft partons cannot affect the rapidity of the Higgs bosons. On the contrary, the radiation of partons that are collinear to p_1 (p_2), i.e., in the forward (backward) region, decreases (increases) the rapidity of the Higgs boson as a consequence of longitudinal-momentum conservation (see Eq. (3)). Since the emissions of collinear partons from p_1 and p_2 are *dynamically* uncorrelated (factorized from each other), correlations arise only from kinematics. The use of the (N_1, N_2)-moments exactly factorizes (see Eqs. (2) and (9)) the kinematical constraint of longitudinal-momentum conservation. It follows that the (N_1, N_2)-dependence of $\mathcal{W}^{(N_1,N_2)}$ is given by the product of two functions (say, $\mathcal{W}^{(N_1,N_2)} = \mathcal{M}_1^{(N_1)}\mathcal{M}_2^{(N_2)}$) that depends only on N_1 or N_2, respectively. If all the partons have the same flavour, the two functions should be equal, and Eq. (14) directly follows from $[\mathcal{W}^{(N_1,N_2)}]_{N_1=N_2=N} = \mathcal{W}_N$.

The formalism illustrated in this section defines a systematic 'order-by-order' (in extended sense) expansion [44] of Eq. (4): it can be used to obtain predictions with uniform perturbative accuracy from the small-q_T region to the large-q_T region. The various orders of this expansion are denoted[4] as LL, NLL + LO, NNLL + NLO, etc., where the first label (LL, NLL, NNLL, ...) refers to the logarithmic accuracy at small q_T and the second label (LO, NLO, ...) refers to the customary perturbative order[5] at large q_T. To be precise, the NLL + LO term of Eq. (4) is obtained by including the functions $g^{(1)}$, $g^{(2)}$ and the coefficient $\mathcal{H}^{(1)}$ (see Eqs. (13) and (12)) in the resummed component, and by expanding the finite (i.e., large-q_T) component up to its LO term. At NNLL + NLO accuracy, the resummed component includes also the function $g_N^{(3)}$ and the coefficient $\mathcal{H}^{(2)}$ (see Eqs. (13) and (12)), while the finite component is expanded up to NLO. It is worthwhile noticing that the NNLL + NLO (NLL + LO) result includes the *full* NNLO (NLO) perturbative contribution in the small-q_T region.

We recall [44] that, due to our actual definition of the logarithmic parameter $\tilde{L}$ in Eq. (10) and to our matching procedure with the perturbative expansion at large q_T, the integral over q_T of the q_T cross section exactly reproduces the customary fixed-order calculation of the total cross section. This feature is not affected by keeping the rapidity fixed. Therefore, the NNLO (NLO) result for total cross section at fixed y is exactly recovered upon integration over q_T of the NNLL + NLO (NLL + LO) q_T spectrum at fixed y.

Within our formalism, resummation is directly implemented, at fixed M_H, in the space of the conjugate variables N_1, N_2 and b. To obtain the cross section in Eq. (2), as function of the kinematical variables s, y and q_T, we have to perform inverse integral transformations. These integrals are carried out numerically. We recall [44] that the resummed form factor (i.e., each of the functions $g^{(k)}(\alpha_S\tilde{L})$ in Eq. (13)) is singular at the value of b where $\alpha_S(\mu_R^2)\tilde{L} = \pi/\beta_0$ (β_0 is the first-order coefficient of the QCD β function). This singularity has its origin from the presence of the Landau pole in the running of the QCD coupling $\alpha_S(q^2)$ at low scales. When performing the inverse Fourier (Bessel) transformation with respect to the impact parameter b (see Eq. (5)), we deal with this singularity by using a 'minimal prescription' [56,57]: the singularity is avoided by deforming the integration contour in the complex b space (see Ref. [57]). We note that the position of the singularity is completely independent of the values of N_1 and N_2. Thus, the inversion of the Mellin moments is performed in the customary way (in Mellin space there are no singularities for sufficiently-large values of $\mathrm{Re}\,N_1$ and $\mathrm{Re}\,N_2$). In this respect, going from single N-moments (as in Ref. [44]) to double (N_1, N_2)-moments (as in the present case, where the rapidity is kept fixed) is completely straightforward, with no additional (practical or conceptual) complications.

3. Higgs boson production at the LHC

In this section we apply the resummation formalism of Section 2 to the production of the Standard Model Higgs boson at the LHC. We closely follow our previous study of the single differential (with respect to q_T) cross section, with the same choice of parameters as stated in Section 3 of Ref. [44]. Therefore, the integration over y of the double differential (with respect to y and q_T) cross sections presented in this section returns the q_T cross sections of Ref. [44]. As a cross-check of the actual implementation of the calculation, we have verified that after integration over the rapidity the numerical results in Ref. [44] are reobtained within a high accuracy.

[4] In the literature on q_T resummation, other authors sometime use the same labels (NLL, NLO and so forth) with a meaning that is different from ours.

[5] We recall that the LO term at small q_T (i.e., including the region where $q_T = 0$) is proportional to α_S^2, whereas the LO term at large q_T is proportional to α_S^3. This mismatch of one power of α_S (and the ensuing mismatch of notation) persists at each higher order (NLO, NNLO, ...).

As in Refs. [17,44], we use an 'improved version' [16] of the large-M_t approximation. The cross section is first computed by using the large-M_t approximation. Then, it is rescaled by a Born level factor, such as to include the exact lowest-order dependence on the masses, M_t and M_b, of the top and bottom[6] quarks, which circulates in the heavy-quark loop that couples to the Higgs boson. We use the values $M_t = 175$ GeV and $M_b = 4.75$ GeV. As discussed in Ref. [17] and recalled in Section 1, this version of the large-M_t approximation is expected to produce an uncertainty that is smaller than the uncertainties from yet uncalculated perturbative terms from higher orders.

For the sake of brevity, we present quantitative results only at NNLL + NLO accuracy, which is the highest accuracy that can be achieved by using the present knowledge of exact perturbative QCD contributions (resummation coefficients and fixed-order calculations [25–27]). We use the MRST2004 set [58] of parton distribution functions at NNLO. The use of NNLO parton densities consistently matches the NNLL (NNLO) accuracy of our partonic cross section in the region of small and intermediate values of q_T.

Resummation up to the NLL level is under control from the knowledge of the perturbative coefficients $A^{(1)}$, $B^{(1)}$, $A^{(2)}$ [35] and $\mathcal{H}^{(1)}$ [37]. To reach the NNLL + NLO accuracy, the form factor function $\mathcal{G}^{(N_1,N_2)}$ in Eq. (13) must include the contribution from $g^{(3)(N_1,N_2)}$ (which is controlled by the coefficients $B^{(2)}$ [38] and $A^{(3)}$ [59]), and the coefficient function $\mathcal{H}^{(N_1,N_2)}$ in Eq. (12) has to be evaluated up to its second-order term $\mathcal{H}^{(2)(N_1,N_2)}$. In Ref. [44] we exploited the unitarity constraint $\mathcal{G}(\alpha_S, \tilde{L})|_{b=0} = 0$ to numerically derive an approximated form of the coefficient $\mathcal{H}^{(2)}$ from the NNLO calculation [12] of the total cross section. The recent calculation of Ref. [15], which is based on the complete evaluation of $\mathcal{H}^{(2)(N_1,N_2)}$ in analytic form, allows us to gauge the quality of the approximated form. We find that the use of the $\mathcal{H}^{(2)}$ of Ref. [44] leads to differences of about 1% with respect to the exact computation of the rapidity cross section at NNLO.

All the numerical results in this section are obtained by fixing the renormalization and factorization scales at the value $\mu_R = \mu_F = M_H$. The 'resummation scale' Q (the auxiliary scale introduced in Ref. [44] to gauge the effect of yet uncalculated logarithmic terms at higher orders) is also fixed at the value $Q = M_H$. The mass of the Higgs boson is set at the value $M_H = 125$ GeV.

We start our presentation of the predictions for Higgs boson production at the LHC by considering the q_T dependence of the cross section at fixed values of the rapidity. In Fig. 1, we set $y = 0$ and we compare the customary (when $q_T > 0$) NLO calculation (dashed line) with the resummed NNLL + NLO calculation (solid line).

As expected, the NLO result diverges to $-\infty$ as $q_T \to 0$ and, at small values of q_T, it has an unphysical peak that is produced by the numerical compensation of negative leading logarithmic and positive subleading logarithmic contributions. The presence of this peak is not accidental. At large q_T, the perturbative expansion at any fixed order has no pathological behaviour: it leads to a positive cross section, whose value decreases as q_T increases. When $q_T \to 0$, instead, any fixed-order calculation diverges alternatively to $\pm\infty$ depending on the perturbative order. Therefore,

[6] We note that the Born level cross section is not insensitive to the contribution of the bottom quark. Adding the bottom-quark loop to the top-quark loop in the scattering amplitude produces a non-negligible interference effect in the squared amplitude. The relative effect of the bottom quark decreases the Born level cross section by about 11% if $M_H = 125$ GeV, and by about 3% if $M_H = 300$ GeV. If $M_H \gtrsim 500$ GeV, the relative effect of the bottom quark is always smaller than 1%.

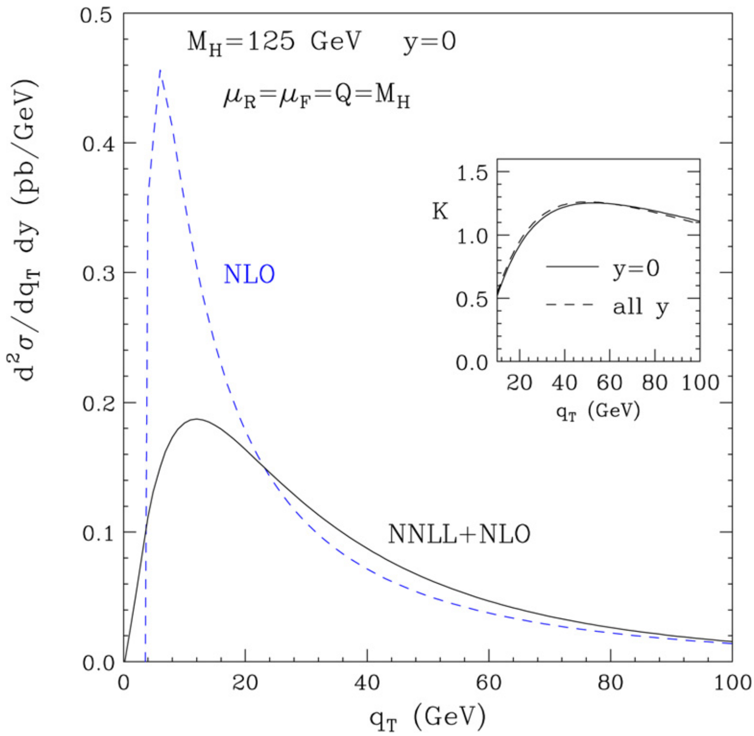

Fig. 1. The q_T spectrum at the LHC with $M_H = 125$ GeV and $y = 0$: results at NNLL + NLO (solid line) and NLO (dashed line) accuracy. The inset plot shows the ratio K (see Eq. (15)) of the corresponding q_T cross sections, fixing $y = 0$ (solid line) and integrating them over the full rapidity range (dashed line).

to go smoothly from the large-q_T behaviour to the small-q_T limit, the NLO (or N^{3}LO, and so forth) calculation of the cross section has to show at least one peak in the intermediate-q_T region.

We recall once more that the label NLO in Fig. 1 refers to (and originates from) the perturbative expansion at large q_T. To avoid possible misunderstandings (coming from such a label) when interpreting the dashed (NLO) curve in the small-q_T region, we point out that, the only difference produced in Fig. 1 by the NNLO calculation at small q_T (this calculation can be carried out, for example, by using the NNLO codes of Refs. [14,15]) is a spike around the point $q_T = 0$. More precisely, *as long as* $q_T \neq 0$, the dashed curve is *exactly* the result of the NNLO calculation of the q_T cross section at small q_T. The only difference introduced in the plot by this NNLO calculation would occur in the first bin (with arbitrarily small size) that includes the point $q_T = 0$. The NNLO value of the q_T cross section in this first bin is positive and fixed by the value of the NNLO total cross section.[7] Of course, owing to the increasingly negative behaviour of the q_T distribution when $q_T \to 0$, the NNLO value of the q_T cross section in the first bin increases by decreasing the size of that bin.

The resummed NNLL + NLO result in Fig. 1 is physically well behaved at small q_T (it vanishes as $q_T \to 0$ and has a kinematical peak at $q_T \sim 12$ GeV), and it converges to the expected NLO result only when q_T is definitely large ($q_T \simeq M_H$).

[7] By definition, the integral over q_T of $d^2\sigma/(dq_T\, dy)$ at NNLO is equal to $d\sigma/dy$ at NNLO.

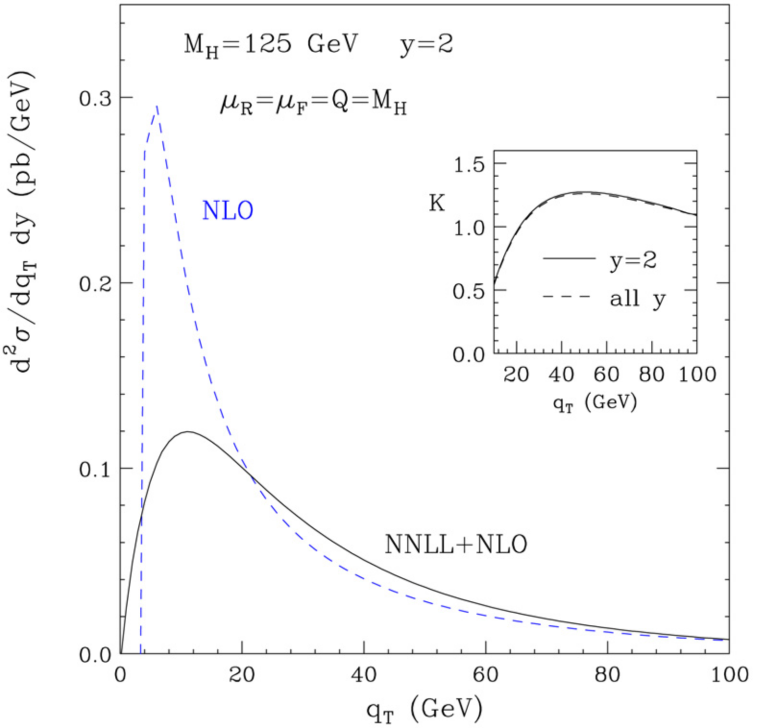

Fig. 2. The q_T spectrum at the LHC with $M_H = 125$ GeV and $y = 2$: results at NNLL + NLO (solid line) and NLO (dashed line) accuracy. The inset plot shows the ratio K (see Eq. (15)) of the corresponding q_T cross sections, fixing $y = 2$ (solid line) and integrating them over the full rapidity range (dashed line).

To quantify more clearly the effect of the resummation on the NLO result, the value at $y = 0$ of the q_T dependent K-factor,

$$K(q_T, y) = \frac{d\sigma_{\mathrm{NNLL+NLO}}/(dq_T\,dy)}{d\sigma_{\mathrm{NLO}}/(dq_T\,dy)}, \tag{15}$$

is shown in the inset plot of Fig. 1. The dashed line shows the analogous K-factor as computed from the ratio of the rapidity integrated cross sections. The similarity between these two K-factors is a first indication of the mild rapidity dependence of the resummation effects. By inspection of the inset plot, we note that NNLL resummation is relevant not only at small q_T, but also in the intermediate-q_T region: as soon as $q_T \lesssim 80$ GeV, the resummation effects are larger than 20%. Of course, the fact that $K \sim 1$ at $q_T \sim 24$ GeV is purely accidental: it simply follows from the unphysical behaviour of the fixed-order perturbative expansion at small q_T.

Considering other values of the rapidity, from the central to the off-central rapidity region, we find the same features as observed at $y = 0$. Our results of the q_T spectrum at $y = 2$ are presented in Fig. 2. The NNLL + NLO spectrum has a peak at $q_T \sim 11$ GeV. As happens in the case of the q_T distribution integrated over y, the effect of NNLL resummation is definitely non-negligible starting from relatively-high values of q_T. For example, at $q_T = 50$ GeV the NNLL + NLO result is about 30% higher than the NLO result.

To analyze the rapidity dependence in more detail, we study the doubly-differential cross section at fixed values of q_T. In Figs. 3 and 4, we show quantitative results at two typical values

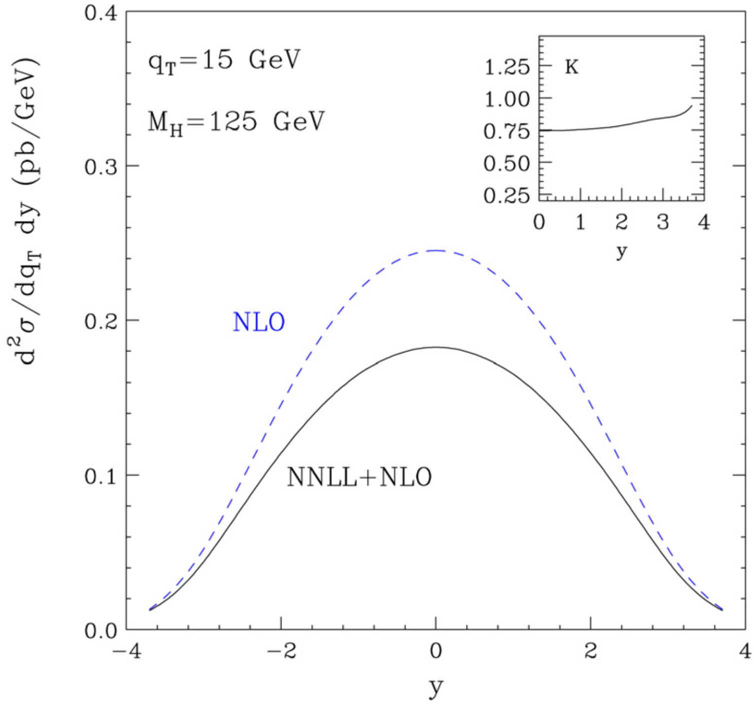

Fig. 3. The rapidity spectrum at the LHC with $M_H = 125$ GeV and $q_T = 15$ GeV: results at NNLL + NLO (solid line) and NLO (dashed line) accuracy. The inset plot shows the K-factor as defined in Eq. (15).

of the transverse momentum, $q_T = 15$ GeV and $q_T = 40$ GeV, in the small-q_T and intermediate-q_T region, respectively.

Fig. 3 shows the rapidity distribution at NNLL + NLO (solid line) and NLO (dashes) accuracy when $q_T = 15$ GeV. At this value of q_T, the effect of NNLL resummation reduces the cross section. For example, when $y = 0$ the reduction effect is about 25%. As can be observed in the inset plot, the relative contribution from the resummed logarithmic terms is rather constant in the central rapidity region, and its dependence on y only appears in forward (and backward) region, where the cross section is quite small.

When $q_T = 40$ GeV (see Fig. 4), instead, the effect of NNLL resummation increases the absolute value of the cross section. For example, when $y = 0$ the NLO cross section is increased by about 22%. Nonetheless, as for the relative effect of resummation and the rapidity dependence of the K-factor, we observe features that are very similar to those in Fig. 3. The resummation effects have a very mild dependence on y in the central and (moderately) off-central regions, and this explains the remarkable similarity between the solid and dashed lines in the inset plot of Figs. 1 and 2. Since the kinematical region where $|y| \lesssim 2$ accounts for most of the total cross section, when comparing the ratio $K(q_T, y)$ to the analogous ratio of the y-integrated cross sections, hardly any differences are expected, unless the large-rapidity region is explored.

The mild rapidity dependence of the q_T shape of the resummed results can be studied with a finer resolution by defining the following ratio:

$$R(q_T; y) = \frac{d^2\sigma/(dq_T\,dy)}{d\sigma/dq_T}. \tag{16}$$

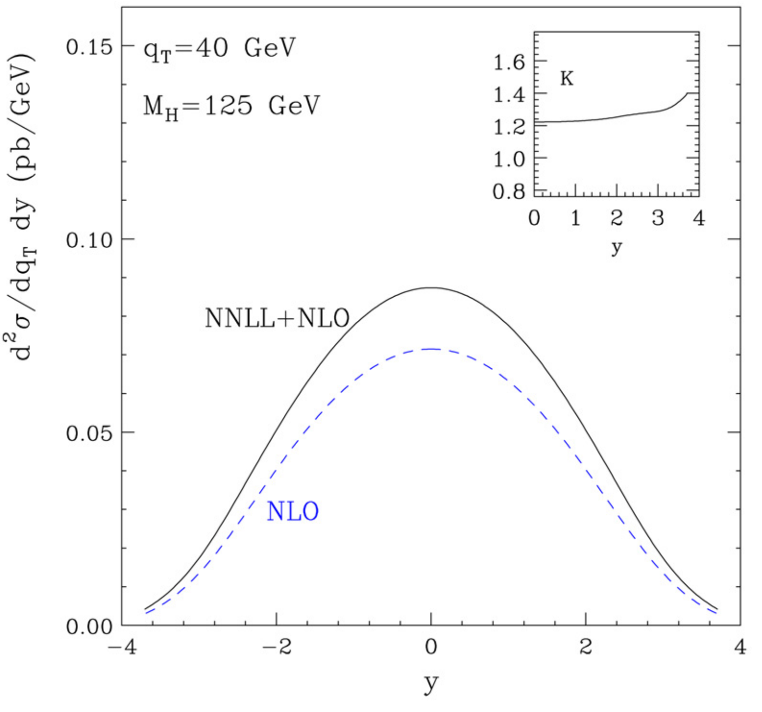

Fig. 4. The rapidity spectrum at the LHC with $M_H = 125$ GeV and $q_T = 40$ GeV: results at NNLL + NLO (solid line) and NLO (dashed line) accuracy. The inset plot shows the K-factor as defined in Eq. (15).

This ratio gives the doubly-differential cross section normalized to the q_T cross section integrated over the full rapidity range. For comparison, we consider also the q_T-integrated version of the cross section ratio in Eq. (16), and we define the ratio

$$R_y = \frac{d\sigma/dy}{\sigma} \tag{17}$$

of the rapidity cross section $d\sigma/dy$ over the total cross section σ.

We have computed the ratio in Eq. (16) by using the resummed q_T cross sections at NNLL + NLO accuracy. The results, as a function of q_T, are presented in Fig. 5 (solid lines) at two different values, $y = 0$ and $y = 2$, of the rapidity. The results of the analogous (q_T-independent) ratio R_y (computed[8] at NNLO with the numerical programs of Refs. [14,15]) at the corresponding values of rapidity are also reported (dotted lines) in Fig. 5. The dashed lines in Fig. 5 correspond to the computation of Eq. (16) by using the q_T cross sections at NLO: we see that the dashed and solid lines are very similar (as expected from the similarity of the dashed and solid lines in the inset plot of Figs. 1 and 2). As discussed below, the results in Fig. 5 show that the cross section decreases and the q_T spectrum softens when the rapidity increases.

[8] The numerical accuracy of this computation is better than about 2%–3%. Owing to the unitarity constraint in our resummation formalism, the same result (with a similar numerical accuracy) can be obtained by integration over q_T of the resummed q_T cross sections.

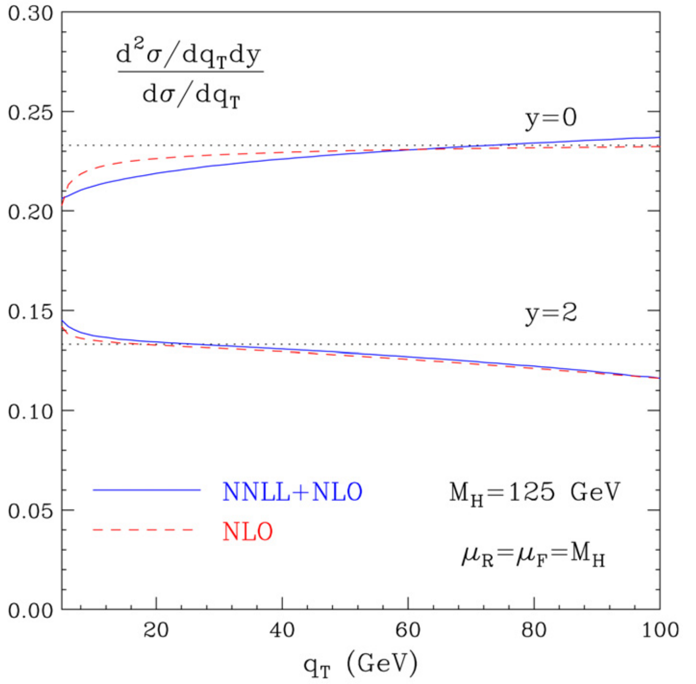

Fig. 5. The rescaled q_T spectrum (as defined by the ratio $R(q_T; y)$ in Eq. (16)) at the LHC with $M_H = 125$ GeV. The solid (dashed) lines correspond to the NNLL + NLO (NLO) results at two different values of the rapidity: $y = 0$ (upper) and $y = 2$ (lower). The dotted lines refer to the corresponding values of the ratio R_y (see Eq. (17)).

We observe that the lines at $y = 0$ lie above the lines at $y = 2$; this is just a consequence of the fact that the cross sections (both at fixed q_T and after integration over q_T) decrease when y increases.

At fixed y, $R(q_T; y)$ is not constant: it depends (though very slightly) on q_T. We note that the corresponding upper and lower lines in Fig. 5 have different slopes with respect to q_T: fixing q_T, the q_T slope of $R(q_T; y)$ decreases from positive to negative values as y increases from $y = 0$ to $y = 2$, thus showing that the q_T spectrum becomes slightly softer at larger rapidity. In general, as $|y|$ increases, the hardness of the q_T shape of $d^2\sigma/(dq_T\, dy)$ decreases. Since the cross section decreases by increasing the rapidity, the hardness of $d\sigma/dq_T$ (the denominator in Eq. (16)) is intermediate between the values of the hardness of $d^2\sigma/(dq_T\, dy)$ (the numerator in Eq. (16)) at $y = 0$ and at large $|y|$. As a consequence, the q_T slope of $R(q_T; y)$ is necessarily positive when $y = 0$. Note that the q_T slope is already negative when $y = 2$ (Fig. 5): this is a consequence of the fact that the bulk of the cross section is in the rapidity region $|y| \lesssim 2$.

Our qualitative illustration of the results in Fig. 5 can be accompanied by some quantitative observations. We note that the rapidity dependence of the cross sections is sizeable: going from $y = 0$ to $y = 2$, the ratio R_y decreases by about 43%; comparable variations affect the ratio $R(q_T; y)$, which is not very different from R_y and it is slowly dependent on q_T. Indeed, at fixed y, the ratio $R(q_T; y)$ at NNLL + NLO accuracy has a small and nearly constant slope from low values of q_T around the peak (say, $q_T \sim 10$ GeV) to $q_T = 100$ GeV; varying q_T in this region, $R(q_T; y)$ increases by about 11% when $y = 0$, and it decreases by about 16% when $y = 2$. In the same range of q_T and y, the values of $R(q_T; y)$ at NNLL + NLO (solid lines) and at NLO (dashed lines) are very similar: although this is expected at large q_T, the differences never exceed the level of about 4% even at values of q_T as low as $q_T \sim 10$ GeV.

In summary, the results in Fig. 5 show that, when $|y|$ increases from the central to the (moderately) off-central region, the cross sections vary more in absolute value than in q_T shape. These features deserve some words of discussion.

We first consider the total cross section σ and the rapidity cross section $d\sigma/dy$. We recall (see Section 1) that the value of these cross sections is sizeably affected by QCD radiative corrections. The bulk of the effect is due to the radiation of virtual and soft gluons, and they cannot affect the rapidity of the Higgs boson. As a consequence, the ratio R_y has little sensitivity to perturbative QCD corrections. The decreases of R_y as $|y|$ increases is mainly driven by the decrease of the gluon density $f_g(x, M_H^2)$ as x increases. Considering the large-q_T region, similar arguments apply to the q_T cross sections $d\sigma/dq_T$ and $d\sigma/(dq_T\,dy)$, and similar conclusions apply to the ratio $R(q_T, y)$. In the small-q_T region, we have to consider the additional and large effect produced on the q_T cross sections by the logarithmically-enhanced terms $\ln^m(M_H^2/q_T^2)$. These terms are due to the radiation of soft and collinear partons. As already discussed in Section 2, the rapidity of the Higgs boson can be varied only by collinear radiation, while soft radiation can only lead to on overall (independent of y) rescaling of the q_T cross sections. At the LL level, only soft radiation contributes (the LL function $g^{(1)}$ in Eq. (13) does not depend on N_1 and N_2) and all the logarithmic terms cancel in the ratio $R(q_T, y)$. The y sensitivity of $R(q_T, y)$ starts at the NLL level. The corrections produced on the dominant soft-gluon effects by the collinear radiation are physically [29] well approximated by varying the scale μ of the gluon density from $\mu \sim M_H$ to $\mu \sim q_T$. As a consequence, the variations of the hardness of the q_T cross sections are mainly driven by $d\ln f_g(x, q_T^2)/d\ln q_T^2$, the amount of scaling violation of the gluon density. Since the scaling violation decreases as x increases, the hardness of $d\sigma/(dq_T\,dy)$ decreases and the q_T spectrum softens as $|y|$ increases. Note that, by increasing x, the gluon density decreases faster than its scaling violation: this explains why $d\sigma/(dq_T\,dy)$ varies more in absolute value than in q_T shape when $|y|$ increases.

We conclude this section with some comments about the theoretical uncertainties on the doubly-differential cross section $d\sigma/(dq_T\,dy)$ at NNLL + NLO accuracy. In Ref. [44] the perturbative QCD uncertainties on $d\sigma/dq_T$ were investigated by comparing the results at NNLL + NLO and NLL + LO accuracies and by performing scale variations at NNLL + NLO level. We also considered the inclusion of non-perturbative contributions, and we found that they lead to small corrections provided q_T is not very small. From these studies we concluded that the NNLL + NLO result has a QCD uncertainty of about $\pm 10\%$ in the region from small (around the peak of the q_T distribution) to intermediate (say, roughly, $q_T \lesssim M_H/3$) values of transverse momenta. Similar studies can be carried out in the case of the doubly-differential cross section $d\sigma/(dq_T\,dy)$. These studies are not reported here since their results and the ensuing conclusions are very similar to those in Ref. [44]. The reason for this similarity is a feature that we have pointed out throughout this section: the q_T resummation effects have a very mild dependence on the rapidity and, thus, they are almost unchanged when comparing $d\sigma/(dq_T\,dy)$ with $d\sigma/dq_T$ (equivalently, they largely cancel in the ratio in the cross section ratio of Eq. (16)).

4. Summary

We have considered the resummation of the logarithmically-enhanced QCD contributions that appear at small transverse momenta when computing the q_T spectrum of a Higgs boson produced in hadron collisions. In our previous work on the subject [41,44], the rapidity of the Higgs boson was integrated over: resummation was implemented by using a formalism based on a transform to impact parameter and Mellin moment space. In this paper we have extended the resummation formalism to the case in which the rapidity is kept fixed, and we have considered the doubly-differential cross section with respect to the transverse momentum and the rapidity. We have shown that this extension can be carried out without substantial complications: it is sufficient to enlarge the conjugate space by introducing a suitably-defined double Mellin transformation.

The main aspects of our method [36,44], which are recalled here, are unchanged by the inclusion of the rapidity dependence. The resummation is performed at the level of the partonic cross section, and the parton densities are factorized as in the customary fixed-order calculations. The formalism is completely general and it can be applied to other processes: the large logarithmic contributions are universal and, thus, they are systematically exponentiated in a process-independent form (see Eqs. (10) and (13)); the process-dependent part is factorized in the hard-scattering coefficient $\mathcal{H}$. A constraint of perturbative unitarity is imposed on the resummed terms (see Eq. (11)), so that the q_T smearing produced by the resummation does not change the total production rate. This constraint reduces the effect of unjustified higher-order contributions at intermediate q_T and facilitates the matching procedure with the complete fixed-order calculations at large q_T. In particular, when the rapidity is kept fixed, the integration over q_T of $d\sigma/(dq_T\,dy)$ at NNLL + NLO accuracy returns $d\sigma/dy$ at NNLO.

We have presented numerical results for Higgs boson production at the LHC. Comparing fixed-order and resummed calculations, we find that the resummation effects are large at small q_T (as expected) and still sizeable at intermediate q_T. The inclusion of the rapidity dependence has little quantitative impact on this picture since, as we have shown, the q_T resummation effects are mildly dependent on the rapidity. Going from the central to the (moderately) off-central rapidity region, the q_T shape of the spectrum slightly softens. In the range from small to intermediate values of q_T, the residual perturbative uncertainty of the NNLL + NLO predictions for $d\sigma/(dq_T\,dy)$ is comparable to that of advanced (NNLO or NNLL + NNLO) calculations of the q_T inclusive cross sections $d\sigma/dy$ and σ.

Acknowledgements

The work of D.dF. was supported in part by CONICET. D.dF. wishes to thank the Physics Department of the University of Florence and INFN for support and hospitality while this work was completed.

Appendix A

In this appendix we present the structure of the resummation formula (10) by explicitly including the dependence on the flavour indices of the colliding partons.

In the context of our resummation formalism, a detailed derivation of exponentiation in the multiflavour case is illustrated in Appendix A of Ref. [44]. Considering a generic LO partonic subprocess $c + \bar{c} \to F$ ($F = H$ and $c = \bar{c} = g$ in the specific case of Higgs boson production by gluon fusion), and performing q_T resummation after integration over the rapidity, the resummed component $d\hat{\sigma}^{(\mathrm{res.})}_{a_1a_2}/dq_T^2$ of the partonic cross section is controlled by the N-moments $\mathcal{W}^F_{a_1a_2,N}$. The final exponentiated result for these N-moments is given by the master formulae (106)–(108) of Ref. [44]. We recall the master formula (106) in the following form:

$$\mathcal{W}^F_{a_1a_2,N}(b, M; \alpha_S) = \sum_{\{I\}} \mathcal{H}^{\{I\},F}_{a_1a_2,N}(M, \alpha_S) \exp\big\{\mathcal{G}_{\{I\},N}(\alpha_S, \tilde{L})\big\}, \tag{A.1}$$

where the sum extends over the following set of flavour indices:

$$\{I\} = c, \bar{c}, i_i, i_2, b_1, b_2, \tag{A.2}$$

and, for simplicity, the functional dependence on various scales (such as the renormalization and factorization scales) is understood. The functions $\mathcal{G}_{\{I\},N}$ and $\mathcal{H}^{\{I\},F}_{a_1a_2,N}$ are given in the master formulae (107) and (108), respectively. In the present paper, q_T resummation is performed at fixed values of the rapidity, and the double (N_1, N_2)-moments $\mathcal{W}^{(N_1,N_2)F}_{a_1a_2}$ in Eq. (6) replace the N-moments $\mathcal{W}^F_{a_1a_2,N}$ of Ref. [44]. The generalization of Eq. (10) to the multiflavour case is straightforwardly obtained from Eq. (A.1) by the simple replacement $N \to (N_1, N_2)$:

$$\mathcal{W}^{(N_1,N_2)F}_{a_1a_2}(b, M; \alpha_S) = \sum_{\{I\}} \mathcal{H}^{\{I\},(N_1,N_2)F}_{a_1a_2}(M, \alpha_S) \exp\bigl\{\mathcal{G}^{(N_1,N_2)}_{\{I\}}(\alpha_S, \tilde{L})\bigr\}. \tag{A.3}$$

The exponent $\mathcal{G}^{(N_1,N_2)}_{\{I\}}$ of the process-independent form factor and the process-dependent hard factor $\mathcal{H}^{\{I\},(N_1,N_2)F}_{a_1a_2}$ are

$$\mathcal{G}^{(N_1,N_2)}_{\{I\}} = \mathcal{G}_c + \mathcal{G}_{i_1,N_1} + \mathcal{G}_{cb_1,N_1} + \mathcal{G}_{i_2,N_2} + \mathcal{G}_{\bar{c}b_2,N_2}, \tag{A.4}$$

$$\mathcal{H}^{\{I\},(N_1,N_2)F}_{a_1a_2} = \sigma^{(0)}_{c\bar{c},F} H^F_c\, S_c \tilde{C}_{cb_1,N_1} \bigl[\boldsymbol{E}^{(i_1)}_{N_1} \boldsymbol{V}^{-1}_{N_1} \boldsymbol{U}_{N_1}\bigr]_{b_1a_1} \tilde{C}_{\bar{c}b_2,N_2} \bigl[\boldsymbol{E}^{(i_2)}_{N_2} \boldsymbol{V}^{-1}_{N_2} \boldsymbol{U}_{N_2}\bigr]_{b_2a_2}. \tag{A.5}$$

The expressions in Eqs. (A.4) and (A.5) are completely analogous to the master formulae (107) and (108) in Ref. [44] (the functional dependence on the scales M, μ_R, μ_F and Q is explicitly denoted in those formulae). In particular, we note that the dependence of $\mathcal{G}^{(N_1,N_2)}$ and $\mathcal{H}^{(N_1,N_2)}$ on the Mellin variables N_1 and N_2 is completely factorized: each of terms on the right-hand side of Eqs. (A.4) and (A.5) depends only on one Mellin variable (either N_1 or N_2). This factorized structure is completely consistent with Eq. (14) and with the physical picture discussed below Eq. (14); the dependence on N_1 (N_2) follows the longitudinal-momentum flow and the flavour flow $a_1 \to b_1 \to i_1 \to c$ ($a_2 \to b_2 \to i_2 \to \bar{c}$) that are produced by collinear radiation from the initial-state parton with momentum p_1 (p_2). The various Mellin functions ($\mathcal{G}_{i,N}, \boldsymbol{E}^{(i)}_N, \boldsymbol{U}_N$ and so forth) in Eqs. (A.4) and (A.5) can be found in Ref. [44].

References

[1] For a review on Higgs physics in and beyond the Standard Model, see J.F. Gunion, H.E. Haber, G.L. Kane, S. Dawson, The Higgs Hunter's Guide, Addison–Wesley, Reading, MA, 1990;
M. Carena, H.E. Haber, Prog. Part. Nucl. Phys. 50 (2003) 63;
A. Djouadi, report LPT-ORSAY-05-17, hep-ph/0503172;
A. Djouadi, report LPT-ORSAY-05-18, hep-ph/0503173.

[2] ATLAS Collaboration, ATLAS Detector and Physics Performance: Technical Design Report, vol. 2, report CERN/LHCC/99-15, 1999;
S. Asai, et al., Eur. Phys. J. C 32 (Suppl. 2) (2004) 19;
CMS Collaboration, CMS Physics Technical Design Report: Physics Performance, vol. 2, report CERN/LHCC/2006-021, 2006.

[3] M. Carena, et al., Report of the Tevatron Higgs working group, hep-ph/0010338;
CDF Collaboration, DØ Collaboration, Results of the Tevatron Higgs Sensitivity Study, report FERMILAB-PUB-03/320-E;
V.M. Abazov, et al., DØ Collaboration, Phys. Rev. Lett. 96 (2006) 011801;
A. Abulencia, et al., CDF Collaboration, Phys. Rev. Lett. 97 (2006) 081802;
The TEVNPH working group, for the CDF and DØ Collaborations, hep-ex/0612044.

[4] S. Dawson, Nucl. Phys. B 359 (1991) 283;
A. Djouadi, M. Spira, P.M. Zerwas, Phys. Lett. B 264 (1991) 440.
[5] M. Spira, A. Djouadi, D. Graudenz, P.M. Zerwas, Nucl. Phys. B 453 (1995) 17.
[6] U. Aglietti, R. Bonciani, G. Degrassi, A. Vicini, JHEP 0701 (2007) 021;
C. Anastasiou, S. Beerli, S. Bucherer, A. Daleo, Z. Kunszt, JHEP 0701 (2007) 082.
[7] M. Muhlleitner, M. Spira, report PSI-PR-06-15, hep-ph/0612254.
[8] R.V. Harlander, Phys. Lett. B 492 (2000) 74;
V. Ravindran, J. Smith, W.L. van Neerven, Nucl. Phys. B 704 (2005) 332;
T. Gehrmann, T. Huber, D. Maitre, Phys. Lett. B 622 (2005) 295.
[9] S. Catani, D. de Florian, M. Grazzini, JHEP 0105 (2001) 025.
[10] R.V. Harlander, W.B. Kilgore, Phys. Rev. D 64 (2001) 013015.
[11] S. Catani, D. de Florian, M. Grazzini, JHEP 0201 (2002) 015.
[12] R.V. Harlander, W.B. Kilgore, Phys. Rev. Lett. 88 (2002) 201801;
C. Anastasiou, K. Melnikov, Nucl. Phys. B 646 (2002) 220;
V. Ravindran, J. Smith, W.L. van Neerven, Nucl. Phys. B 665 (2003) 325.
[13] C. Anastasiou, L.J. Dixon, K. Melnikov, Nucl. Phys. B (Proc. Suppl.) 116 (2003) 193.
[14] C. Anastasiou, K. Melnikov, F. Petriello, Phys. Rev. Lett. 93 (2004) 262002;
C. Anastasiou, K. Melnikov, F. Petriello, Nucl. Phys. B 724 (2005) 197.
[15] S. Catani, M. Grazzini, Phys. Rev. Lett. 98 (2007) 222002.
[16] M. Kramer, E. Laenen, M. Spira, Nucl. Phys. B 511 (1998) 523.
[17] S. Catani, D. de Florian, M. Grazzini, P. Nason, JHEP 0307 (2003) 028.
[18] S. Moch, A. Vogt, Phys. Lett. B 631 (2005) 48.
[19] E. Laenen, L. Magnea, Phys. Lett. B 632 (2006) 270.
[20] A. Idilbi, X.d. Ji, J.P. Ma, F. Yuan, Phys. Rev. D 73 (2006) 077501.
[21] V. Ravindran, Nucl. Phys. B 746 (2006) 58;
V. Ravindran, Nucl. Phys. B 752 (2006) 173;
V. Ravindran, J. Smith, W.L. van Neerven, report HRI-04-2006, hep-ph/0608308.
[22] R.K. Ellis, I. Hinchliffe, M. Soldate, J.J. van der Bij, Nucl. Phys. B 297 (1988) 221;
U. Baur, E.W. Glover, Nucl. Phys. B 339 (1990) 38.
[23] V. Del Duca, W. Kilgore, C. Oleari, C. Schmidt, D. Zeppenfeld, Nucl. Phys. B 616 (2001) 367;
V. Del Duca, W. Kilgore, C. Oleari, C.R. Schmidt, D. Zeppenfeld, Phys. Rev. D 67 (2003) 073003.
[24] J. Smith, W.L. van Neerven, Nucl. Phys. B 720 (2005) 182.
[25] D. de Florian, M. Grazzini, Z. Kunszt, Phys. Rev. Lett. 82 (1999) 5209.
[26] V. Ravindran, J. Smith, W.L. Van Neerven, Nucl. Phys. B 634 (2002) 247.
[27] C.J. Glosser, C.R. Schmidt, JHEP 0212 (2002) 016.
[28] D. de Florian, A. Kulesza, W. Vogelsang, JHEP 0602 (2006) 047.
[29] Y.L. Dokshitzer, D. Diakonov, S.I. Troian, Phys. Lett. B 79 (1978) 269;
Y.L. Dokshitzer, D. Diakonov, S.I. Troian, Phys. Rep. 58 (1980) 269.
[30] G. Parisi, R. Petronzio, Nucl. Phys. B 154 (1979) 427.
[31] G. Curci, M. Greco, Y. Srivastava, Nucl. Phys. B 159 (1979) 451.
[32] J.C. Collins, D.E. Soper, Nucl. Phys. B 193 (1981) 381;
J.C. Collins, D.E. Soper, Nucl. Phys. B 213 (1983) 545, Erratum;
J.C. Collins, D.E. Soper, Nucl. Phys. B 197 (1982) 446.
[33] J. Kodaira, L. Trentadue, Phys. Lett. B 112 (1982) 66;
J. Kodaira, L. Trentadue, report SLAC-PUB-2934, 1982;
J. Kodaira, L. Trentadue, Phys. Lett. B 123 (1983) 335.
[34] J.C. Collins, D.E. Soper, G. Sterman, Nucl. Phys. B 250 (1985) 199.
[35] S. Catani, E. D'Emilio, L. Trentadue, Phys. Lett. B 211 (1988) 335.
[36] S. Catani, D. de Florian, M. Grazzini, Nucl. Phys. B 596 (2001) 299.
[37] R.P. Kauffman, Phys. Rev. D 45 (1992) 1512;
C.P. Yuan, Phys. Lett. B 283 (1992) 395.
[38] D. de Florian, M. Grazzini, Phys. Rev. Lett. 85 (2000) 4678;
D. de Florian, M. Grazzini, Nucl. Phys. B 616 (2001) 247.
[39] C. Balazs, C.P. Yuan, Phys. Lett. B 478 (2000) 192;
C. Balazs, J. Huston, I. Puljak, Phys. Rev. D 63 (2001) 014021.
[40] E.L. Berger, J.w. Qiu, Phys. Rev. D 67 (2003) 034026;
E.L. Berger, J.w. Qiu, Phys. Rev. Lett. 91 (2003) 222003.

[41] G. Bozzi, S. Catani, D. de Florian, M. Grazzini, Phys. Lett. B 564 (2003) 65.
[42] A. Kulesza, W.J. Stirling, JHEP 0312 (2003) 056.
[43] A. Kulesza, G. Sterman, W. Vogelsang, Phys. Rev. D 69 (2004) 014012.
[44] G. Bozzi, S. Catani, D. de Florian, M. Grazzini, Nucl. Phys. B 737 (2006) 73.
[45] Q.H. Cao, C.R. Chen, report UCRHEP-T428, arXiv: 0704.1344.
[46] A. Gawron, J. Kwiecinski, Phys. Rev. D 70 (2004) 014003;
G. Watt, A.D. Martin, M.G. Ryskin, Phys. Rev. D 70 (2004) 014012;
G. Watt, A.D. Martin, M.G. Ryskin, Phys. Rev. D 70 (2004) 079902, Erratum;
M. Luszczak, A. Szczurek, Eur. Phys. J. C 46 (2006) 123.
[47] G. Davatz, G. Dissertori, M. Dittmar, M. Grazzini, F. Pauss, JHEP 0405 (2004) 009.
[48] A.V. Lipatov, N.P. Zotov, Eur. Phys. J. C 44 (2005) 559.
[49] F. Stockli, A.G. Holzner, G. Dissertori, JHEP 0510 (2005) 079;
G. Davatz, F. Stockli, C. Anastasiou, G. Dissertori, M. Dittmar, K. Melnikov, F. Petriello, JHEP 0607 (2006) 037.
[50] C. Anastasiou, G. Dissertori, F. Stockli, report CERN-PH-TH/2007-118, arXiv: 0707.2373.
[51] S. Catani, L. Trentadue, Nucl. Phys. B 327 (1989) 323;
S. Catani, L. Trentadue, Nucl. Phys. B 353 (1991) 183.
[52] H. Kawamura, J. Kodaira, K. Tanaka, hep-ph/0703079.
[53] G. Sterman, W. Vogelsang, JHEP 0102 (2001) 016.
[54] S. Catani, L. Trentadue, G. Turnock, B.R. Webber, Nucl. Phys. B 407 (1993) 3.
[55] G. Sterman, Nucl. Phys. B 281 (1987) 310.
[56] S. Catani, M.L. Mangano, P. Nason, L. Trentadue, Nucl. Phys. B 478 (1996) 273.
[57] E. Laenen, G. Sterman, W. Vogelsang, Phys. Rev. Lett. 84 (2000) 4296;
A. Kulesza, G. Sterman, W. Vogelsang, Phys. Rev. D 66 (2002) 014011.
[58] A.D. Martin, R.G. Roberts, W.J. Stirling, R.S. Thorne, Phys. Lett. B 604 (2004) 61.
[59] A. Vogt, S. Moch, J.A.M. Vermaseren, Nucl. Phys. B 691 (2004) 129.